A Measurement of Coherent J/Ψ Electro-production Off ^{4}He in Hall C

W. Armstrong, I. Cloët, S. Joosten, J. Kim, T.-S. H. Lee, Z.-E. Meziani, C. Peng, J. Xie

Physics Division, Argonne National Laboratory, Argonne, IL 60439, USA

M. Jones

Jefferson Lab, Newport News, VA 23606, USA

A Letter of Intent to PAC48

Abstract

In this letter we propose to measure for the first time the matter form factor of ^{4}He across a wide range of t through coherent electro-production of J/ψ on a high pressure gas ^{4}He target in Hall C at Jefferson Lab. Using the highest possible CEBAF beam energy available in Hall C, we will attempt to extract a gluonic matter form factor of ^{4}He by performing a measurement of the reaction ^{4}He(e,e$'$ ^{4}He)J/ψ where the J/ψ is reconstructed via invariant mass. The coincidence measurement of a scattered electron and recoiling nucleus will use both spectrometers, HMS and SHMS, to detected scattered electrons. Significant kinematic coverage in t is enabled through the recoil detection of ^4He, leaving the J/ψ decay undetected. A new tracking detector will reconstruct the recoiling ^4He momentum vector starting at kinetic energies of 40 MeV. An existing 20 cm race-track pressurized ^{4}He gas target with roughly half the density as liquid helium will be used with 11 GeV incident electron beam energy at 50 μA beam current. The measured cross section will be used to extract the matter form factor which will be compared with the latest lattice calculations. The proposed measurements, together with lattice QCD predictions, are the first step towards the first ever extraction of a gluonic radius. This experiment will be a precursor to the possible complete studies on ^{4}He that can be performed at an EIC.

Contents

Introduction & Motivation

In nuclear physics the description of a nucleus is usually expressed in terms of the hadronic degrees of freedom. Most commonly, it is described using nucleons and their interactions, mediated by light mesons for the long range part of the nucleon-nucleon interaction, multi-pions and heavier mesons for the intermediate region, and a phenomenological repulsive part at short distance. Ab-initio calculations using hadronic degrees of freedom have been very successful in describing the ground state of light nuclei for example. However, at a deeper level it is still puzzling how to relate the success of this nucleon-meson description to the basic degrees of freedom of QCD, quarks and gluons, and their direct role in the emerging properties of a nucleus.

More recently, with the keen desire to understand nuclear physics in terms of QCD, questions about the explicit role of quarks and gluons in nuclei have taken center stage. Ab initio calculations of basic properties of light nuclei using lattice QCD have been initiated, albeit with approximations due to the limited performance of the best available computers. Novel supercomputers such as quantum computers as well as enhanced computing methods are our best future promise to ultimately tackle this problem with the controlled approximations. In the mean time experiments could help provide an answer to some simple but important questions in this regard.

One of the fundamental puzzles in hadronic physics is the origin of the nucleon mass. *How does the mass emerge from the relative contributions by the quarks and gluons?* An important piece of this puzzle can be gleaned from nature the matter radius of the nucleon, and its relative magnitude compared to the charge radius. The nature of the gluonic radius of a nucleus is a similar puzzling question in nuclear physics. Is the gluonic radius of ^{4}He larger or smaller than the charge radius of ^{4}He? While we understand that the charge radius of a nucleus emanates from the average motion and dynamical properties of the charged quarks it is not obvious what role the gluons play in defining the matter radius of the nucleus. While the charge distribution of many nuclei has been measured through electron scattering and charge radii have been extracted from their form factors, one has yet to understand the matter distribution, which must involve the gluons and is therefore not easily accessible by electron scattering.

From a nucleonic picture for the description of nuclei, the charge form factor of ^{4}He exhibits at least two diffractive minima [1] due to bound nucleons distributing their charge in the nucleus (see Figure 1.1). Switching to the partonic picture, charged quarks must form

nucleon clumps leading to the formation of the first diffractive minimum in $|F_c|(Q^2)$. But will gluonic matter clump identically and form a similar diffractive structure in the matter form factor? Will the gluonic matter have diffractive minima at the same values of Q^2, if any at all? The proposed experiment will address this last question by measuring the production cross section over a wide range of t centered on the charge form factor's first diffractive minimum.

In summary, coherent electro-production of J/ψ on ^{4}He offers a unique opportunity to, for the first time, explore the gluonic component of its matter distribution directly. Lattice calculations at the partonic level of the matter form factor in ^{4}He in the measured region will be a powerful benchmark test of QCD in nuclei. With this experiment we will have a preview of the gluonic form factor of ^{4}He. We will need first to benckmark first lattice QCD calculations of ^{4}He in the measured range and then extend the calculations to extract the radius from the data and lattice calculations in the unmeasured region. It is also a precursor of the possibilities of similar studies at an EIC.

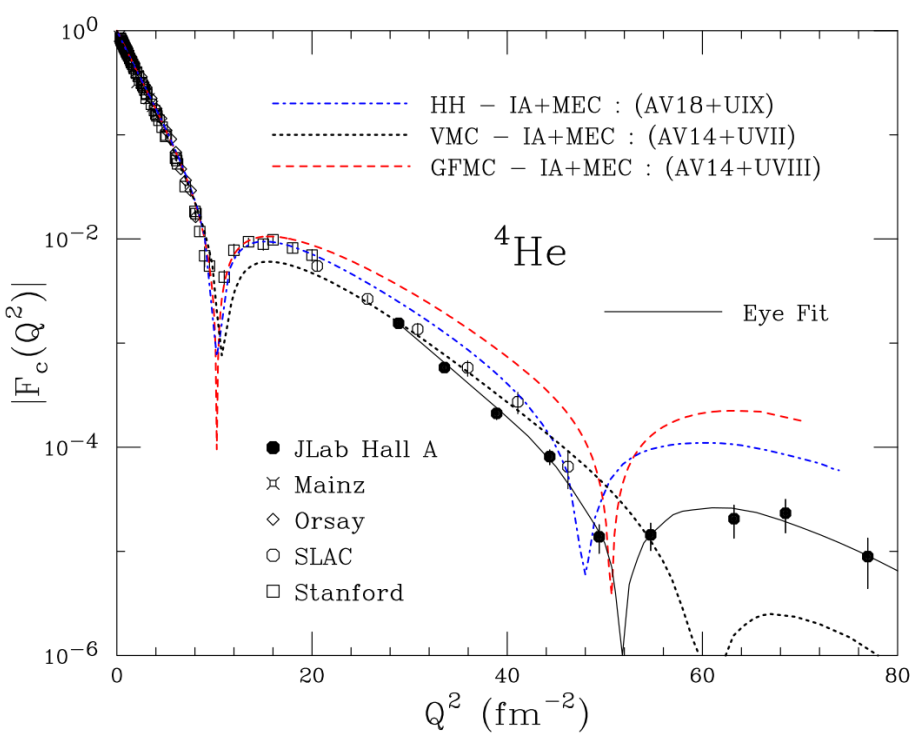

Figure 1.1: The charge form factor of ^{4}He with the second diffractive minimum confirmed by measurements at JLab [1].

Theory Evaluations

2.1 Theory Model

With the objective to show that in principle the experiment is feasible and determine our beam time request we chose the Pomeron-Exchange model developed in Ref. [2, 3] to evaluate the cross sections. We then merged these cross sections into our simulation to make experimental predictions for the proposed experiment.

Using the factorization approximation within the multiple scattering formulation, the differential cross section of exclusive photo-production of J/ψ on a nuclear target (T) with A nucleons, $\gamma(q) + T(P_i) \longrightarrow J/\psi(k) + T(P_f)$ can be written as

$$\frac{d\sigma}{dt} = \frac{\pi}{|\vec{q}||\vec{k}|}\left(\frac{d\sigma}{d\Omega_{Lab}}\right) \tag{2.1}$$

where the differential cross section in the laboratory frame ($\vec{P}_i = 0$) is

$$\frac{d\sigma}{d\Omega_{Lab}} = \frac{(2\pi)^4|\vec{k}|^2 E_{J/\psi}(\vec{k})E_T(\vec{q}-\vec{k})}{|E_T(\vec{q}-\vec{k})|\vec{k}| + E_{J/\psi}(\vec{k})(|\vec{k}| - |\vec{k}|\cos\theta_{Lab})|} \tag{2.2}$$

$$\times \quad |AF_T(t)|^2 \times \left[\frac{1}{4}\sum_{m_s,\lambda_\gamma}\sum_{m'_s,\lambda_{J/\psi}}\right]|\langle k\lambda_{J/\psi}; p_f m'_s|T_{\mathbb{P}}|q\lambda'_\gamma p_i m_s\rangle|^2 \tag{2.3}$$

where $t = (q-k)^2$, $\cos\theta_{Lab} = \hat{q}\cdot\hat{k}$ and $\langle k\lambda_{J/\psi}; p_f m'_s|T_{\mathbb{P}}|q\lambda'_\gamma p_i m_s\rangle$ is the matrix element of the Pomeron exchange in the nucleon photo-production of J/ψ, $\gamma(q) + N(p_i) \to J/\psi(k) + N(p_f)$.

Here $F_T(t)$, the matter form factor is related to the nuclear charge form factor $F_c(t)$ with no exchange current contributions as

$$F_c(t) = F_N(q^2)F_T(q^2 = t) \tag{2.4}$$

Given that the process is fully exclusive, the largest photo-production cross sections will be reached when t is small enough such that the matter form factor of ^{4}He is not too small and thus t is close to t_{min} while t_{min} itself is smallest. To get a sense of the dependence of t_{min} with the photon beam energy and also what momenta of J/ψ and ^{4}He are probed we show this dependence in Fig.2.2

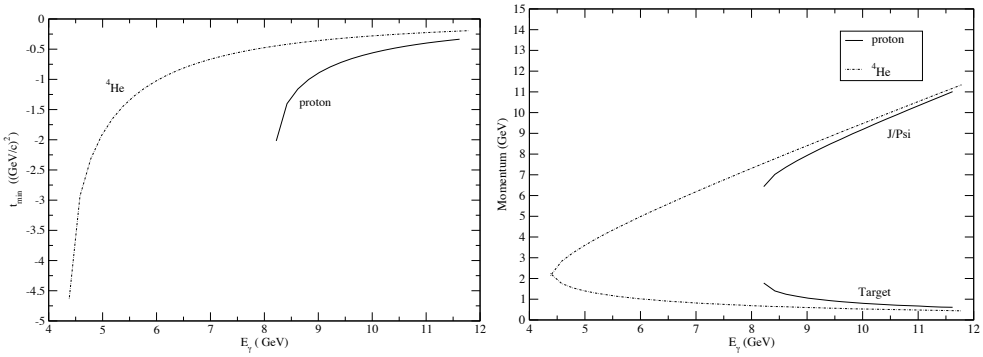

Figure 2.2: Left: Variation of t_{min} for coherent photo-production of J/ψ on a proton and a ^{4}He from threshold to 11.5 GeV photon beam. Right: Momenta of outgoing J/ψ and ^{4}He as a function of photon beam energy.

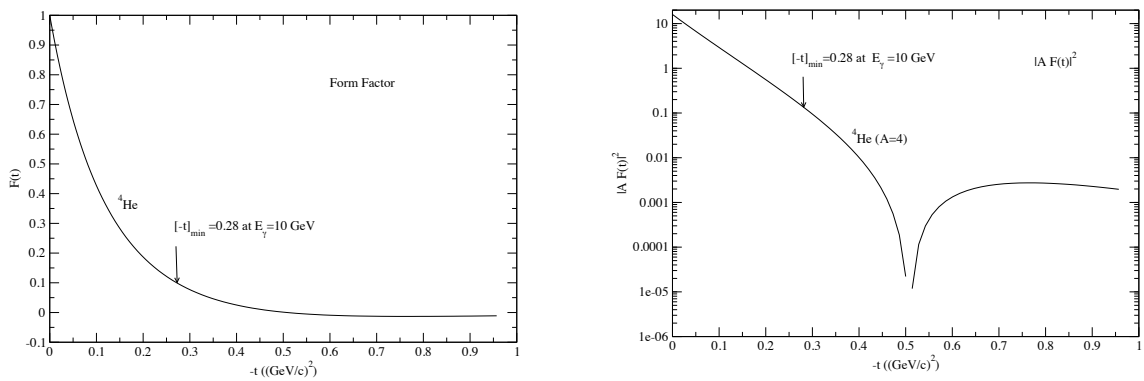

Figure 2.3: Left: Matter form factor as a function of $-t$ of ^{4}He generated in Ref. [4]. Right: $|AF(t)|^2$ using the same form factor.

2.2 Theory cross sections estimates

Using the formalism above, with the matter form factor shown in Fig.2.3, the differential cross section was evaluated at different bremsstrahlung beam energies from 8.5 GeV where t is about 0.5 GeV^2 to less then 0.25 GeV^2 at 11 GeV photon beam energy.

It is clear that given the t-dependence of the matter form factor, and the fact that the higher the photon beam energy the lower the accessible t_{min}, we have an opportunity to measure a differential cross section equivalent to that measured on the proton at photon energies close to the maximum electron beam energy of about 11.0 GeV. An estimation of the differential cross section at different photon beam energies, using the model above, is shown in Fig. 2.4.

The total coherent photo-production cross section on ^{4}He is shown along that on a proton

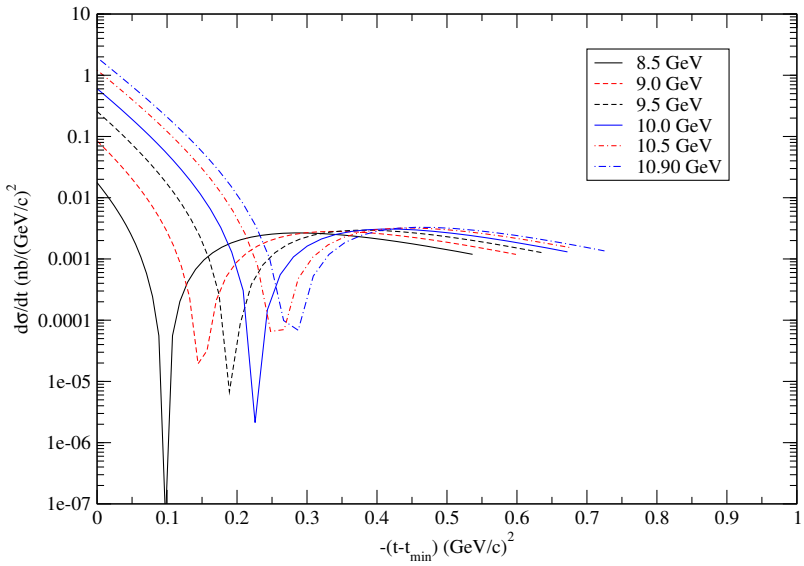

Figure 2.4: Differential cross section $-(t-t_{min})$ dependence for several photon energies well above the coherent threshold production of J/ψ on ^{4}He. Note that the higher the energy the higher the overall differential cross section

for comparison in Fig. 2.5. The size of this total cross section is dominated by the low t values of the differential cross section. The change in slope as the photon energy becomes larger reflects the relative contribution when t_{min} is above or below the first diffraction minimum in the cross section.

2.3 Electro-production Cross Section

The exclusive lepto-production cross section for ^{4}He(e,e$'$ ^{4}He)J/ψ is estimated by the Vector Meson Dominance (VMD) model [5], given as

$$\sigma_{el}(Q^2) = \int_{-t_{max}}^{t_{min}} dt \frac{d\sigma(t,Q^2)}{dt} \cdot \left(\frac{M_{J/\psi}^2}{Q^2 + M_{J/\psi}^2} \right)^m \cdot (1 + \varepsilon R(Q^2)), \tag{2.5}$$

where $d\sigma/dt$ is the aforementioned photo-production cross section, $m = 2.575$ from the fit to HERMES data [6]. Here $R = \sigma_L/\sigma_T$ for vector meson production is given by the parameterization as

$$R(Q^2) = \left(\frac{cM_{J/\psi}^2 + Q^2}{cM_{J/\psi}^2} \right)^n - 1, \tag{2.6}$$

with $c = 2.164$ and $n = 2.131$ from Ref. [7].

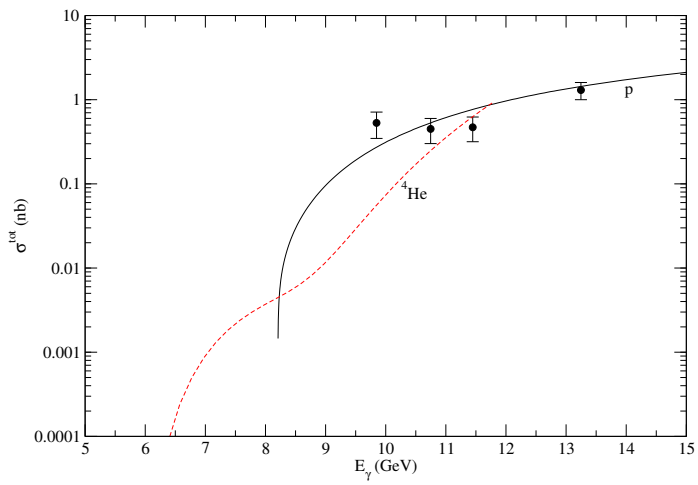

Figure 2.5: Total cross section of coherent J/ψ on ^{4}He (dashed curve). The solid curve is that of the proton for comparison. The data points are part of SLAC and Cornell near threshold proton measurements. GlueX recent data on the proton are not shown here

2.4 Kinematics

Based on the estimated electro-production cross sections, the kinematics distribution of recoiled ^{4}He and scattered electrons from ^{4}He(e,e$'$ ^{4}He)J/ψ with 11 GeV beam is shown in Fig. 2.6. Note the photo-production cross section used in the simulation has a cut-off on $-t$ at around 1 GeV^2. Since the "photon equivalent energy", defined as $k_\gamma = E_{beam} - E'_{el} - Q^2/2M_{^4\mathrm{He}}$, increases with the decrease of Q^2 and E'_{el}, the rates from electro-production are maximized at small scattering angle and low scattered electron energy.

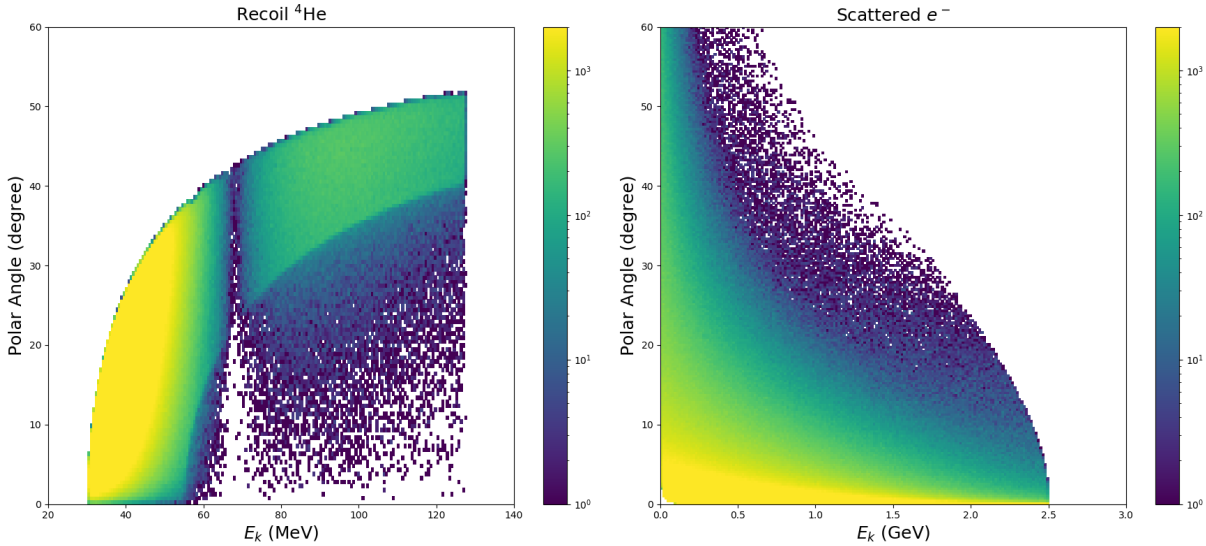

Figure 2.6: Polar angle and kinetic energy distribution of recoil ^{4}He nuclei and scattered electrons. The simulated events assumed the beam energy at 11 GeV and 30 days of beam time.

Proposed Measurement in Hall C

The proposed experiment will measure the reaction ^{4}He(e,e$'$ ^{4}He)J/ψ using both spectrometers in Hall C and an additional 2π recoil detector. The recoil ^{4}He detector is yet to be determined, but it will be designed to reconstruct the recoiling ^{4}He angle and energy starting with the lowest kinetic energy of 40 MeV. A 20 cm high pressure ^{4}He gas target and a beam current of 50 µA will achieve a luminosity of $6 \times 10^{37}\text{cm}^{-2}\text{s}^{-1}$ which presents new instrumentation challenges discussed in the follow sections. The experimental setup is shown in Figure 3.7.

3.1 Beam and Target Configuration

First, an incident electron beam energy of 11 GeV and a 50 µA beam current will be used for most data production. Table 3.1 shows a result of a GEANT simulation where the target density is assumed to be 0.06 g/cm^2 and an aluminum side wall thickness of 0.26 mm. The recoiling ^{4}He is transported through the target and wall material for various recoil kinetic energies.

The target requirements are (i) high luminosity operation and (ii) lowest possible momentum ^{4}He recoil detection. Generally, requirement (i) pushes the target densities higher, however, requirement (ii) favors lower densities to limit the energy loss of recoiling ^{4}He as they exit the target. Balancing these requirements, we assumed a cold gas target with half the density of a helium target previously used for measurements of elastic scattering from ^{4}He at JLab [1]. The previous target system was 20 cm long with 0.5 mm side walls, pressurized to 14 atm at 8 K, and operated with densities of 0.102 g/cm^3 to 0.127 g/cm^3 (just above liquid helium). We also assume that the aluminum walls are half the thickness in the GEANT4 simulation since the target is running at half the pressure.

3.2 Detectors

3.2.1 Recoil Detector

From the results shown in Table 3.1 we see that recoils with $T_{\text{recoil}} = 40$ MeV exit the surface of the target walls having already lost almost half their kinetic energy. With a very

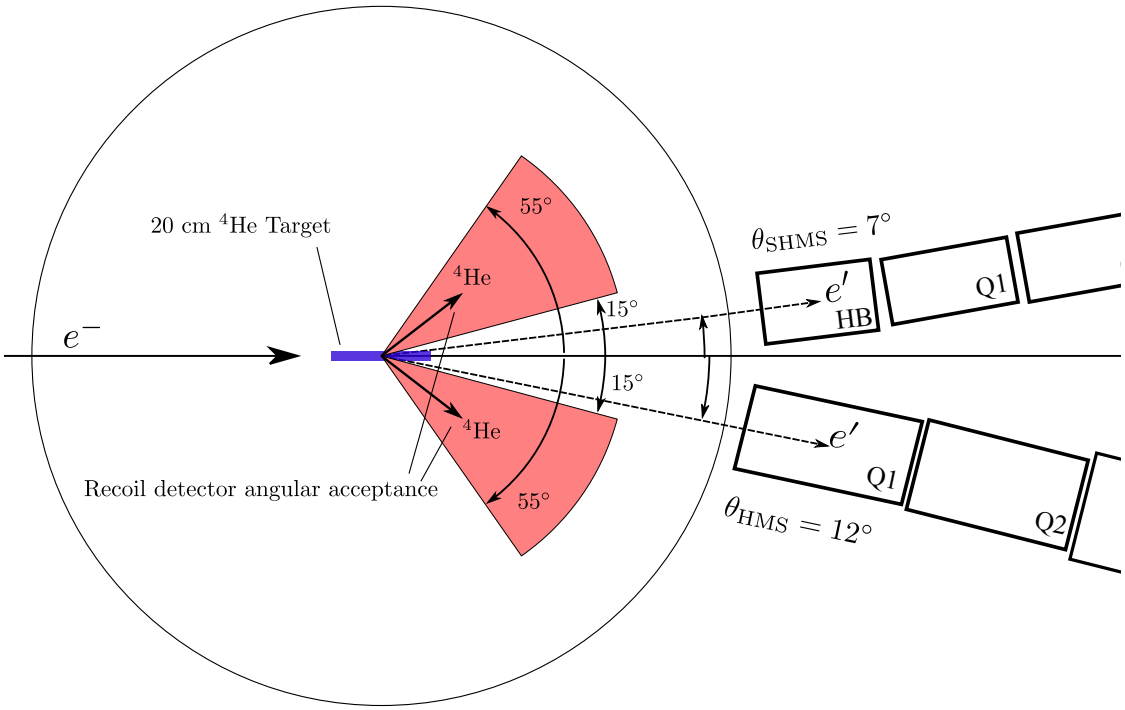

Figure 3.7: The experimental setup in Hall C. Note this diagram is not to scale.

Table 3.1: Energy loss of the ^{4}He recoil in the target, assuming a high-density gas target at 50% of the liquid density, and a target wall of 0.26 mm Al. The simulation was performed using GEANT. For momenta larger than 500MeV, more than 99.7% of ^{4}He will make it out of the target with reasonable kinetic energy.

T_{recoil} MeV	$\mathrm{P}_{\mathrm{recoil}}$ GeV/c	Exit eff. %	T_{exit} (peak) MeV
30.5	0.480	85.4	1-2
33.0	0.499	99.7	10.2
36.0	0.521	99.8	16.5
39.0	0.543	99.6	21.5
42.0	0.563	99.6	26.2
45.0	0.583	99.6	30.4
50.0	0.615	99.6	36.9
55.0	0.645	99.9	43.2
60.0	0.674	99.6	49.2
70.0	0.729	99.6	60.6

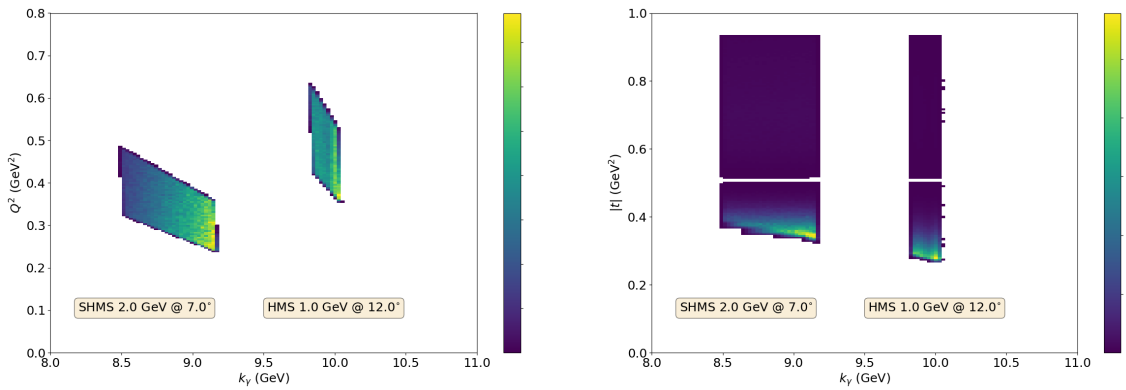

Figure 3.8: Phase space for the electro-production process weighted by the cross section model described in the above sections. Left: Accepted phase space of Q^2 vs. k_γ; Right: Accepted phase space of $|t|$ vs. k_γ.

strong Bragg peak, these α particles will require very little further material to stop. For this reason small detectors close to the target with minimal material between the vertex and sensitive detector element is best (for example see [8]).

As can be seen in Figure 3.7, the recoil detector will be just outside of the spectrometer acceptances. Here it will have to survive in a high radiation environment and operate at high rates.. Additionally, we will want to have the detector as close to the target as possible which adds another problem: a cryogenic target. Another requirement is to have good time resolution, ideally < 500 ps to further reduce the accidental background.

One novel detector scenario which addresses these challenges (high rates, radiation, cryogenic temperatures) is using superconducting nanowire detectors inside of the target cell. Recent R&D has shown superconducting nanowire detectors can operate in high magnetic fields [9] and we believe these detectors to be very rad hard. Although the technology is still being developed for application in nuclear physics, it shows tremendous potential as a tracking detector for this experiment. Another scenario is to use silicon detectors around the target. These can for a cone covering the recoil angles shown inf Figure 3.7. We will continue to investigate possible detectors for a full proposal.

3.2.2 Singles and DAQ Rates

With the two spectrometers at relatively small angles and low momentum the rates in each arm will be significant. These low Q^2 settings present a high rate to the drift chambers of the HMS and SHMS. Conservative estimates for singles rates from different processes are shown in Table 3.2. We are investigating options for upgrading the SHMS and HMS detector stacks because the drift chambers which suffer from tracking inefficiencies and HV trips at high rates.

With the detectors able to operate efficiently at these singles rates, the coincidence trigger

	SHMS (kHz)	HMS (kHz)
inclusive π^-	1100	1600
quasi-elastic radiative tail	308	35
DIS	45	4
Others	<1	<1
Total	1453	1639

Table 3.2: Singles rate estimates from various processes for the two spectrometer settings.

rate can now be estimated. We assume the Cherenkov detectors are in the trigger to eliminate most of the pion events. This coincidence rate is estimated to be roughly 1.2 kHz with a 50 ns trigger window. An offline coincidence timing cut of 1 ns will reduce this accidental rate to 25 Hz.

3.3 Simulation of rates for the measurement

The simulation used is similar to that of the proton experiment E12-16-007 performed in Hall C Ref. [10] except that the target is ^{4}He and the cross section model is that described above in this letter. In this experiment, because the form factor of ^{4}He drops dramatically, it is important to optimize the setup to measure a t distribution in a range close to the lowest value of t_{min} that is accessible. Shown in Fig. 3.8 is the accepted phase spaces for the corresponding HMS/SHMS setting and the recoil ^{4}He detection within $15^\circ < \theta_{\rm He} < 55^\circ$, weighted by the electro-production cross sections. The selected kinematic settings allow us to get a reasonable amount of events within 30 days of a 50 μA electron beam on a 20 cm high pressure ^{4}He target. The reconstructed missing mass and t in the accepted phase spaces are shown in Figure 3.9 and Figure 3.10.

The measurement requires coincidence detection of the recoil ^{4}He nuclei and scattered electrons. Provided the PAC finds the physics case compelling we intend to design such a system for a future proposal. Many possibilities are under consideration, including silicon detectors and nanowire detectors, but we are not in a position to offer a serious design at this time.

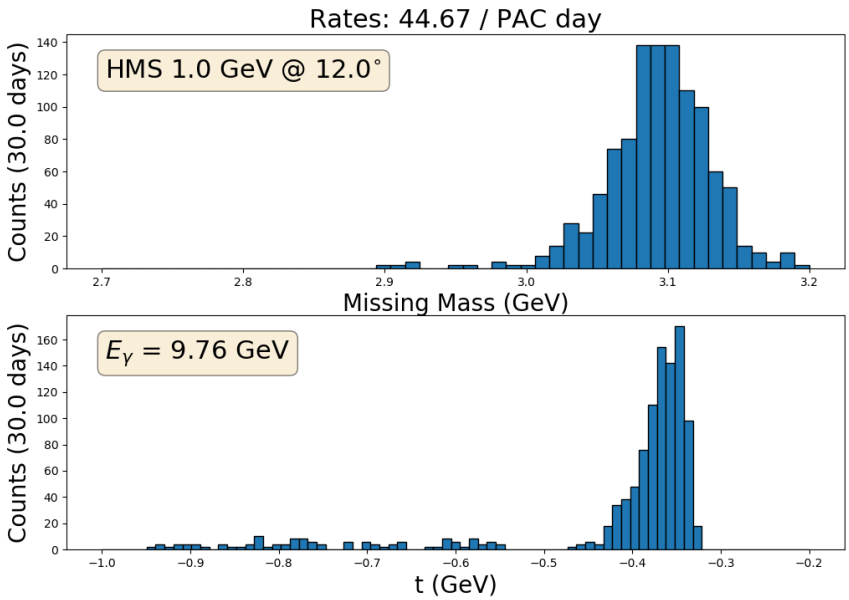

Figure 3.9: Reconstructed kinematic variables for HMS.

3.4 Projected Results and Discussion

We show in Figure 3.11 and Figure 3.12 the projected results with 30 days of beam time and the proposed detector settings. These results show the beneficial wide t range covered through proposed measurement technique, which pushes the rate capabilities of detectors in the spectrometers and requires new recoil detectors to be developed.

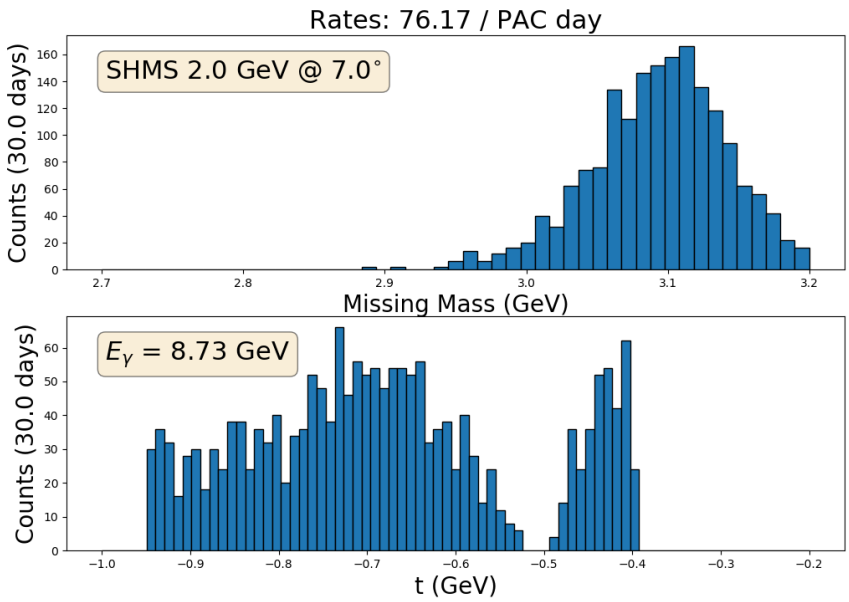

Figure 3.10: Reconstructed kinematic variables for SHMS.

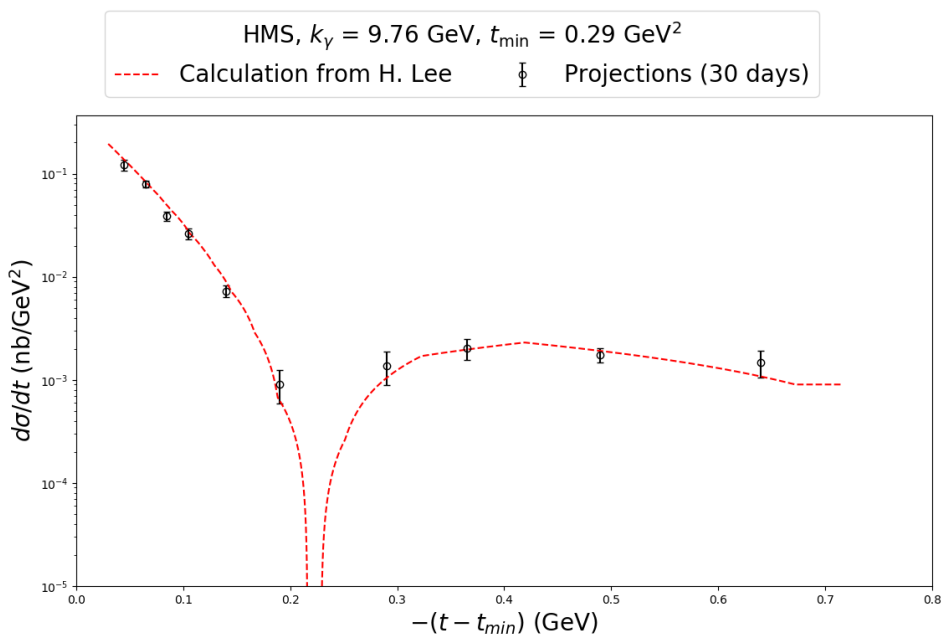

Figure 3.11: Unfolded t dependence of the differential cross sections for HMS data sets. The dashed curve is given by the model described earlier.

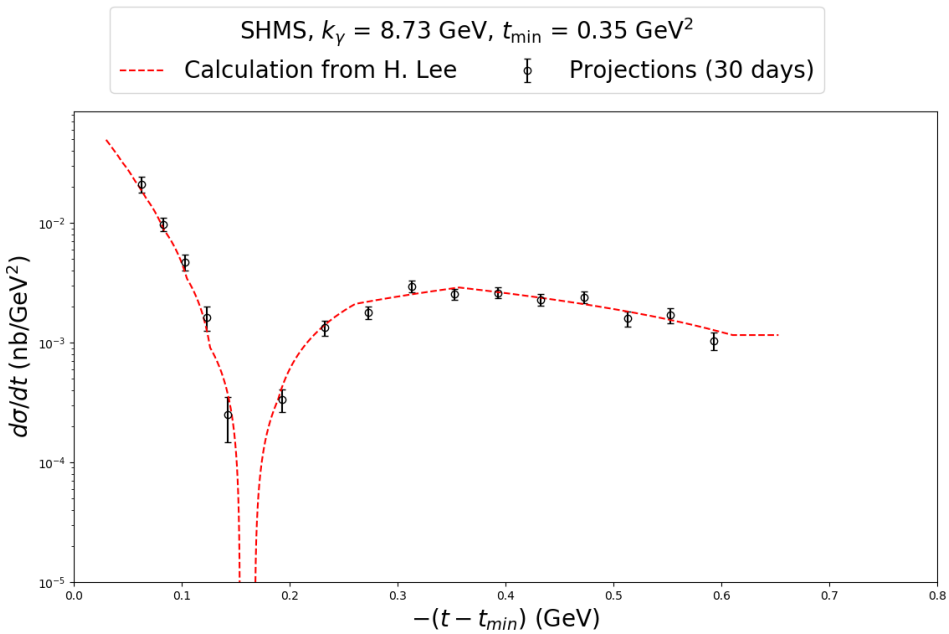

Figure 3.12: Unfolded t dependence of the differential cross sections for SHMS data sets. The dashed curve is given by the model described earlier.

Summary

We presented in this letter of intent a motivation and possible feasibility of measuring the coherent electro-production cross section of J/ψ mesons off ^{4}He in a wide range t with the goal of comparing the matter form factor with lattice calculations and attempting for the first time to extract the gluonic radius of ^{4}He. The experiment requires 30 days of a 50μA electron beam on a 20 cm long ^{4}He gas target. The HMS and SHMS detect the scattered electrons in coincidence with a recoiling ^{4}He nucleus where the J/ψ decay goes undetected. For such a process, a new recoil detector which operates at high rates near the target is needed. Furthermore, upgrades to the HMS and SHMS tracking detectors are required to run at the desired luminosities and compete the measurement in 30 days.

Starting from a partonic picture for the description of nuclei, little is known about the gluonic form factor of ^{4}He, especially without evoking a system of bound nucleons who's charge distribution generate the diffractive minima seen in the charge form factor, $|F_c|$. With broad coverage in t, this experiment will span the first diffractive minimum and be the first to identify a corresponding diffractive minimum in the gluonic matter form factor. Such an observation will impact our understanding of how gluons distribute themselves in nuclei. *Is gluonic matter distributed in the same proportions as charged quarks in nuclei?* A stepping stone towards future studies at an EIC, this experiment challenges our understand of ^{4}He in the nucleonic picture, which was used as an approximation in our model of the estimated rates. This proposed measurement in combination with modern lattice predictions of the ^{4}He nucleus matter form factor will be critical for a deeper understanding of the partonic picture of this tightly bound nuclear system.

Bibliography

[1] A. Camsonne *et al.*, "JLab Measurement of the ^{4}He Charge Form Factor at Large Momentum Transfers," *Phys. Rev. Lett.*, vol. 112, no. 13, p. 132503, 2014.

[2] Y.-s. Oh and T. S. H. Lee, "One-loop corrections to omega photoproduction near threshold," *Phys. Rev.*, vol. C66, p. 045201, 2002.

[3] J.-J. Wu and T. S. H. Lee, "Photo-production of Bound States with Hidden Charms," *Phys. Rev.*, vol. C86, p. 065203, 2012.

[4] R. B. Wiringa, "Variational calculations of few-body nuclei," *Phys. Rev.*, vol. C43, pp. 1585–1598, 1991.

[5] M. Adams *et al.*, "Diffractive production of $\rho^0(770)$ mesons in muon proton interactions at 470-GeV," *Z. Phys. C*, vol. 74, pp. 237–261, 1997.

[6] M. Tytgat, "Diffractive production of ρ^0 and ω vector mesons at HERMES," Ph.D. dissertation, Hamburg U., 2001.

[7] R. Fiore, L. Jenkovszky, V. Magas, S. Melis, and A. Prokudin, "Exclusive J/Psi electroproduction in a dual model," *Phys. Rev. D*, vol. 80, p. 116001, 2009.

[8] W. R. Armstrong *et al.*, "Spectator-Tagged Deeply Virtual Compton Scattering on Light Nuclei," *arXiv*, 8 2017.

[9] T. Polakovic, W. Armstrong, V. Yefremenko, J. Pearson, K. Hafidi, G. Karapetrov, Z.-E. Meziani, and V. Novosad, "Superconducting nanowires as high-rate photon detectors in strong magnetic fields," *Nucl. Instrum. Meth. A*, vol. 959, p. 163543, 2020.

[10] Z. E. Meziani *et al.*, "A Search for the LHCb Charmed 'Pentaquark' using Photo-Production of J/ψ at Threshold in Hall C at Jefferson Lab," *JLab Proposal*, 2016.